The Journal of Supercritical Fluids 215 (2025) 106413

Contents lists available at ScienceDirect

The Journal of Supercritical Fluids

journal homepage: www.elsevier.com/locate/supflu

Micronization of ciprofloxacin by the Supercritical Antisolvent (SAS) Technique

Fouad Zahran [c], Pablo Marzal [a], Helga K. Ruiz [a,b,1], Eduardo Pérez [a], Lourdes Calvo [b], Albertina Cabañas [a,*]

[a] Physical Chemistry Department, Universidad Complutense de Madrid, Spain
[b] Chemical Engineering and Materials Department, Universidad Complutense de Madrid, Spain
[c] Chemistry Department, Faculty of Science, Helwan University, Cairo, Egypt

HIGHLIGHTS

- CIP and CIP·HCl have been micronized by SAS at 40–60 °C and 100–150 bar.
- The crystal structure of SAS samples changed compared to the starting material.
- CIP and CIP·HCl SAS samples show an acicular morphology (1–4 μm long).
- Addition of excipients (lactose or PVP) led to flakes, sheets or globular particles.
- The antibacterial activity of the SAS samples was confirmed.

GRAPHICAL ABSTRACT

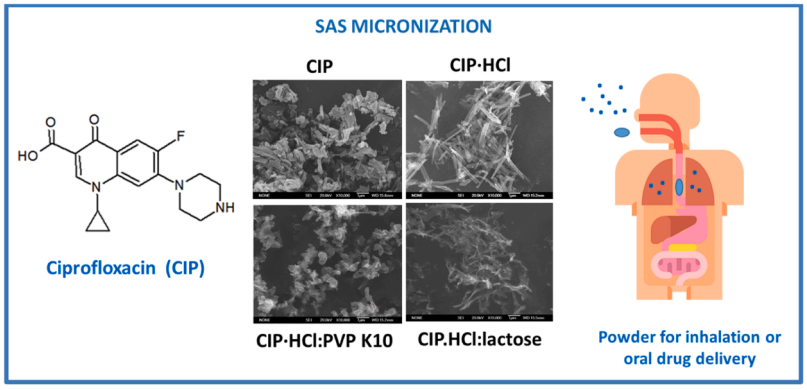

ARTICLE INFO

Keywords:
Drug delivery
Supercritical CO_2
Supercritical fluids
Micronization
Antisolvent

ABSTRACT

Ciprofloxacin is a broad-spectrum antibiotic that is proposed for pulmonary administration. In this work micronization of ciprofloxacin was performed by the Supercritical Antisolvent Technique (SAS) using ciprofloxacin base (CIP) in ethanol/acetic acid and ciprofloxacin hydrochloride salt (CIP·HCl) in methanol at 40–60 °C and 100–150 bar. Yields ranged from 40 % to 90 %. CIP precipitated incorporating acetate whilst CIP·HCl precipitated as the AH1 anhydrous form. CIP and CIP·HCl particles exhibited an acicular morphology (0.2–0.9 μm wide × 1–4 μm long). Micronization adding lactose, PVP K-10 and K-30 modified the precipitate morphology. CIP·HCl:lactose and CIP·HCl:PVP K-30 at a 4:1 drug:excipient mass ratio precipitated like flakes. CIP·HCl:PVP K-10 precipitated as submicron globular particles suitable for oral formulation. Increasing the PVP content, the morphology changed to sheets and flakes, which could be used for pulmonary administration. The antibacterial activity of the samples for *Staphylococcus epidermidis* was confirmed.

* Corresponding author.
E-mail address: a.cabanas@quim.ucm.es (A. Cabañas).
[1] https://orcid.org/0000-0003-2575-1233

https://doi.org/10.1016/j.supflu.2024.106413
Received 2 July 2024; Received in revised form 16 September 2024; Accepted 16 September 2024
Available online 17 September 2024

1. Introduction

Ciprofloxacin is a broad-spectrum antibiotic that belongs to the fluoroquinolone family, with activity against many gram-positive and some gram-negative bacteria. The bactericidal action of ciprofloxacin is due to the inhibition of some enzymes necessary for the replication, transcription, repair, and recombination of bacterial DNA [1]. Ciprofloxacin is prescribed for the treatment of infections in the respiratory, urinary, genital and gastrointestinal tracts; also in intra-abdominal, osteoarticular, skin and soft tissue infections, conjunctivitis, and otitis, among others [2]. Within respiratory tract infections, ciprofloxacin is indicated in bronchopulmonary infections in cystic fibrosis or bronchiectasis, pneumonia, and in exacerbations of chronic obstructive pulmonary disease [3,4]. It is marketed as a single drug in the form of tablets, ear drops, eye drops, ophthalmic ointment, oral suspension and solution for infusion [2]. It is also used as ear drops associated with corticosteroids, such as hydrocortisone and fluocinolone acetonide [5].

The bioavailability of ciprofloxacin from oral delivery is 69 % as it distributes into other tissues [6]. Severe symptoms associated with ciprofloxacin toxicity due to overdose have been reported [7]; this constitutes a good reason to develop ways to reduce the dose of the drug to be administered. Micronization of the drug leads to a reduction in the particle drug size, which modifies the pharmacokinetic and pharmacodynamic properties of the drug, improves its bioavailability and solubility and consequently reduces the drug's adverse effects [8].

The pharmacokinetic properties of ciprofloxacin and its antibacterial effect make it a drug of choice for treating pathologies using the inhalation route [9]. This route enhances the microbial effect, allows for reduction of the dose, reduces sputum volume and purulence, and reduces systemic exposure due to their local action, avoiding systemic side effects [3,8,10]. Furthermore, it provides a very fast absorption rate, due to the low amount of metabolic enzymes present in the lungs and the avoidance of hepatic first-pass metabolism [11,12]. The dose of the drug deposited in the lungs and its distribution determines the therapeutic effect and this distribution depends on the drug particle size, the inhalation device and its use. The recommended particle size for dry powder inhalation is between 1 and 5 μm because this size allows a deeper distribution in the airways, causing a better therapeutic response. Thus, micronization of the drug needs to be performed.

Ciprofloxacin molecule contains two ionizable groups (Fig. 1), the carboxylic and a secondary amine groups, which determine the behaviour of the drug depending on the pH. At acidic pH, ciprofloxacin acquires a positive charge whilst at a higher pH the drug exists as a neutral-charge zwitterion, which is practically insoluble in water.

There are at least two different forms of commercialized pure solid ciprofloxacin drug: ciprofloxacin base (CIP) and ciprofloxacin hydrochloride hydrate (CIP·HCl). CIP is in the zwitterion form whilst CIP·HCl appears in the cationic form. At the pH found in the lungs (pH ~ 7.4), the different ciprofloxacin forms may exhibit different residence times. In particular, the use of CIP will have a longer residence time in the lungs compared to CIP·HCl [13,14].

Ciprofloxacine dry powder formulations have been previously prepared by different techniques [15]. A formulation formed by CIP·HCl and colistin sulfate has been prepared by ball milling achieving particle sizes lower than 5.6 μm [16]. Ciprofloxacin nanocrystal-containing liposomes prepared by freeze-thaw have been also spray dried with sucrose, magnesium stearate and isolecitine leading to ca. 1 μm particles [17]. Similarly, Ciprofloxacin has been micronized with dimyristoyl phosphatidylglycerol and lactose by spray-freeze drying obtaining particles of 2.8 μm [18].

Furthermore, two ciprofloxacin inhalation formulations, a dry powder and a liposomal formulation, are in different stages of clinical development. PulmoSpher™ technology of Novartis Pharma AG uses the dry powder at a dose of 32.5 mg every 12 hours. The liposomal formulation from Aradigm Corp., CA, has two forms, Lipoquin®, which contains the liposomal ciprofloxacin, and Pulmaquin®, which combines the liposomal and free formulation and contains 150 mg of ciprofloxacin in 3 mL of the solution. Both formulations are administered once a day [8,10,14].

PulmoSphere™ formulation uses a spray drying process to produce a dried powder. It is composed of small crystalline particles of ciprofloxacin 3.5 hydrate, which is the zwitterionic form of the drug crystallized in water at neutral pH, coated with a porous layer of distearoylphosphatidylcholine (DSPC) and $CaCl_2$ in 2:1 mol ratio [14].

However, due to the widespread use of this antibiotic, the development of ciprofloxacin alternative formulations is of great interest. Supercritical fluids have attracted a lot of interest in the micronization of different drugs [19]. They have liquid-like densities with gas-like transport properties. Furthermore, their properties can be adjusted with small changes in pressure and temperature. CO_2 is the fluid most commonly used for micronization because of its mild critical temperature and pressure, 31.0 °C and 7.38 MPa, making it suitable for processing heat-sensitive compounds. It is cheap, non-flammable, non-toxic, recyclable, inert and chemically stable and it is considered a Generally Recognized as Safe (GRAS) solvent. Moreover, as it is a gas under normal conditions, it can be eliminated by lowering the pressure, leaving no residue in the product. Supercritical CO_2 ($scCO_2$) is also easily recycled [20,21]. Depending on the solubility of the drug in the supercritical fluid and organic solvents, different micronization techniques can be applied [19,22,23].

When the drug is insoluble in $scCO_2$, the Supercritical Antisolvent Technique (SAS) can be used. In the SAS process, a solution of the drug in an organic solvent is injected into a chamber containing CO_2 at supercritical conditions. $scCO_2$ mixes with the organic solvent and induces the precipitation of the drug [24]. This method has been extensively used in the preparation of microparticles and nanoparticles of different drugs with very good control of the particle size distribution [22]. The elimination or reduction of the use of toxic organic solvents and the morphological and crystallographic control of the precipitated particles are the main advantages of this method. Oftentimes the drug is coprecipitated with different excipients, sometimes polymers, to improve the properties of the micronized powders [24–26]. The formation of drug cocrystals has been also extensively studied [27]. The use of supercritical fluids in the micronization of ciprofloxacin has not been previously reported.

The solubility of CIP in supercritical CO_2 is very low with a maximum

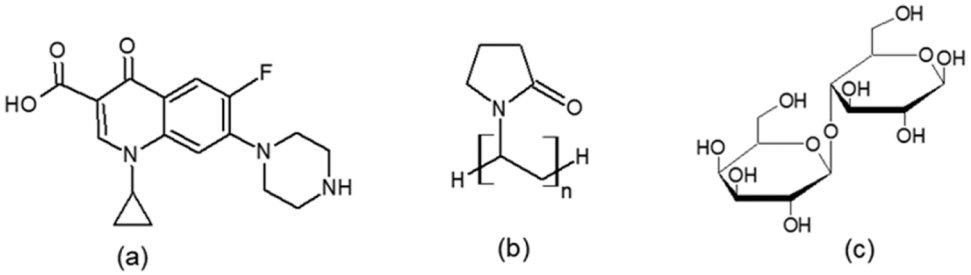

Fig. 1. Structure of ciprofloxacin (a) and the excipients PVP (b) and lactose (c).

mole fraction solubility value of 1.887 10^{-7} at 60 ºC and 360 bar [28]. Although not informed, the solubility of CIP·HCl (hydrochloride ciprofloxacin salt) in $scCO_2$ is expected to be low. On the other hand, CIP is highly insoluble in water at neutral pH (zwitterion form) (0.067 mg/mL) and practically insoluble in ethanol (0.046 mg/mL) [29]. However, it can be easily dissolved in dilute hydrochloric acid and acetic acid solutions [2]. The solubility of this compound in ethanol can be greatly improved up to almost 3 mg/mL by the addition of a small amount of acetic acid. In contrast, CIP·HCl is more soluble in water (cationic form) (30 mg/mL) and exhibits some solubility in ethanol (0.117 mg/mL)[30] and in methanol (> 4 mg/mL). Both ethanol and methanol are fully miscible with CO_2 at moderate pressure and temperature conditions [31]. Then both CIP and CIP·HCl are suitable candidates to be micronized by SAS.

Lactose monohydrate is approved by the FDA for inhalation therapy of dry powders and is considered the excipient of choice for carrier-based dry powder inhalation. It is used as a bulking agent to improve powder fluidity, necessary for filling, device emptying and drug deposition [32]. Polyvinylpyrrolidone (PVP) is an inert, non-toxic, temperature-resistant, pH-stable, biocompatible, biodegradable, and water-soluble polymeric excipient [33] that it is also approved in the pharmaceutical, biomedical and food industries. PVP has been extensively used in the preparation of micro and nanoparticles to decrease particle aggregation and induce amorphization of the drug by different micronization techniques including those based on the use of supercritical CO_2 [34–37]. PVP has also been used in an inhaled dosage form of an anticancer drug demonstrating excellent aerosolization performance and improved therapeutic potential [38].

In this paper, the micronization of CIP and CIP·HCl by the Supercritical Anti-Solvent (SAS) technique is assessed. CIP was dissolved in a mixture of ethanol with 2 % v/v acetic acid, whilst CIP·HCl was micronized from a methanol solution. To improve the properties of the precipitates and control their particle morphology, micronization of CIP·HCl with different excipients, PVP and lactose (whose structure is shown in Fig. 1) was also performed.

The materials obtained were thoroughly characterized using standard material characterization techniques. Their antibacterial activity was also evaluated against *Staphylococcus epidermidis* and compared to a standard Ciprofloxacin base. *Staphylococcus epidermidis* is a gram-positive bacterium and is one of the main representatives of the microbiota of human skin and mucous membranes.

2. Material and methods

2.1. Chemicals and reagents

The drugs and excipients employed were ciprofloxacin $C_{17}H_{18}FN_3O_3$ (ACROS Organics, 98 mol%), ciprofloxacin hydrochloride hydrate (Fisher, 98 mol%), polyvinylpyrrolidone (PVP) K-10 (average mw. 10,000) and K-30 (average mw. 40,000) and d(+)-Lactose 1-hydrate $C_{12}H_{22}O_{11}·H_2O$ (Panreac). Ethanol (Scharlau, ≥ 99.9 mol%), methanol (Fisher, ≥ 99.8 mol%) and acetic acid (Fisher, ≥ 99.9 mol%) were used as solvents and additives. CO_2 (99.995 mol% pure) was provided by Carburos metálicos, Spain.

In the antimicrobial activity assays the reagents employed were: meat extract (Scharlau), casein tryptic peptone (Tryptone, Scharlau), sodium chloride (Panreac, 99 mol% pure), peptone from soybean meal (Fluka), d(+)-Glucose anhydrous (Scharlau), di-potassium hydrogen phosphate (Panreac) and buffered peptone water 0.1 % (Scharlau). Strains of *Staphylococcus epidermidis* (CECT 231; ATCC 12228; CIP 68.21; DSM 1798) were bought from the Spanish Collection of Type Cultures (CECT).

All reagents were used as received without further purification.

2.2. Supercritical Anti-Solvent (SAS) precipitation

A schematic diagram of the SAS apparatus used in the micronization of ciprofloxacin is shown in Fig. 2**.** A complete description of the high-pressure equipment can be found in previous reports [39,40].

The equipment consisted of two pumps to introduce CO_2 (Thar-SCFP-50) and the liquid solution (Lab Alliance Series III Pump) into a 500 mL stainless steel precipitation chamber (Thar instrument) which was heated by a heating band connected to a PID controller. A Back Pressure Regulator (BPR, Thar-SCF ABPR-20) at the end of the line, kept the pressure of the system constant. After the BPR, a cyclonic separator collected the liquid solvent, whilst the CO_2 was evacuated. The rig was protected from possible blockages with check valves, rupture disks and relief valves placed conveniently in the system.

In a typical experiment chilled CO_2 (-10ºC) was pumped continuously at 20 g/min and preheated to the working temperature before entering the precipitation chamber at a constant temperature. When the selected pressure was reached and the system was at stationary conditions, ca. 50 mL of the solution containing the drug dissolved into the organic solvent (ethanol or methanol) was pumped at 1.5 mL/min and injected into the precipitation chamber co-currently with the CO_2 through a 100 μm nozzle to generate small droplets. The CO_2 caused a volumetric expansion of the droplet solvent and a reduction of its solvation powder, leading to a sudden supersaturation and consequently precipitation of the drug in the form of a fine powder. The precipitate was collected in a stainless steel basket placed into the precipitation chamber equipped with a 0.2 μm nylon filter over a 2 μm steel frit at the bottom. Once the liquid pump was stopped, 1.5 L of CO_2 at the precipitation conditions (three times the volume of the chamber) was allowed to flow through the chamber to remove the solvent from the precipitate. CO_2 and the depleted solution went through the BPR and separated in the cyclone separator at atmospheric pressure.

The solution with CIP at 1.5 mg/mL was prepared dissolving ca. 75 mg of ciprofloxacin base weighed in an analytical balance (A&D GR-200, ± 0.1 mg) in 50 mL of ethanol with 2 % v/v acetic acid. For the micronization of CIP·HCl in methanol, a 2 mg/mL solution was used. The micronization experiments of CIP·HCl with excipients (PVP K-10, PVP K-30 and lactose) were performed at 4:1, 2:1 and 1:1 drug to excipient mass ratios, at a total concentration of CIP·HCl equal to 2.5 mg/mL. Before pumping the solution into the reactor, the solution was preheated in a water bath on a hot stirring plate (Fisher Scientific Isotemp, ± 0.1 ºC) to the selected precipitation temperature.

Experiments were performed at a temperature between 40 and 60ºC and a pressure between 100 and 150 bar. The operation conditions were selected to achieve full miscibility of the solvents (ethanol or methanol) and CO_2 in the chamber [31]. Experiments were performed in duplicate or triplicate, being very reproducible. Precipitation yield was estimated from the amount recovered only in the basket and it can be considered a lower limit as very small particles may have escaped through the filter out of the basket. An uncertainty in the yield of 10 % was estimated.

2.3. Materials characterization

X-ray diffraction (XRD) patterns of the composite materials were collected using a XPERT MPD diffractometer with Cu Kα radiation at 2θ values between 5º and 30º. Xpert Highscore program with PFDF-4+2023 database was used for identification. Fourier Transfer Infrared (FTIR) spectra of the materials were recorded using Perkin Elmer apparatus with an Attenuated Total Reflection (ATR) attachment at a spectral resolution of 4 cm^{-1} between 4000 and 650 cm^{-1}. Elemental analysis was performed on a LECO CHNS-932 microanalyser. The uncertainties in the elemental analysis were %C ± 0.26, %H ± 0.24, %N ± 0.25 and %S ± 0.35. The amount of ciprofloxacin in the SAS precipitates along with the excipients (PVP K-10, PVP K-30 and lactose) was determined by UV–vis using an Agilent Cary 8454 spectrophotometer. The calibration curve was prepared using the CIP base starting material in HCl 0.1 M.

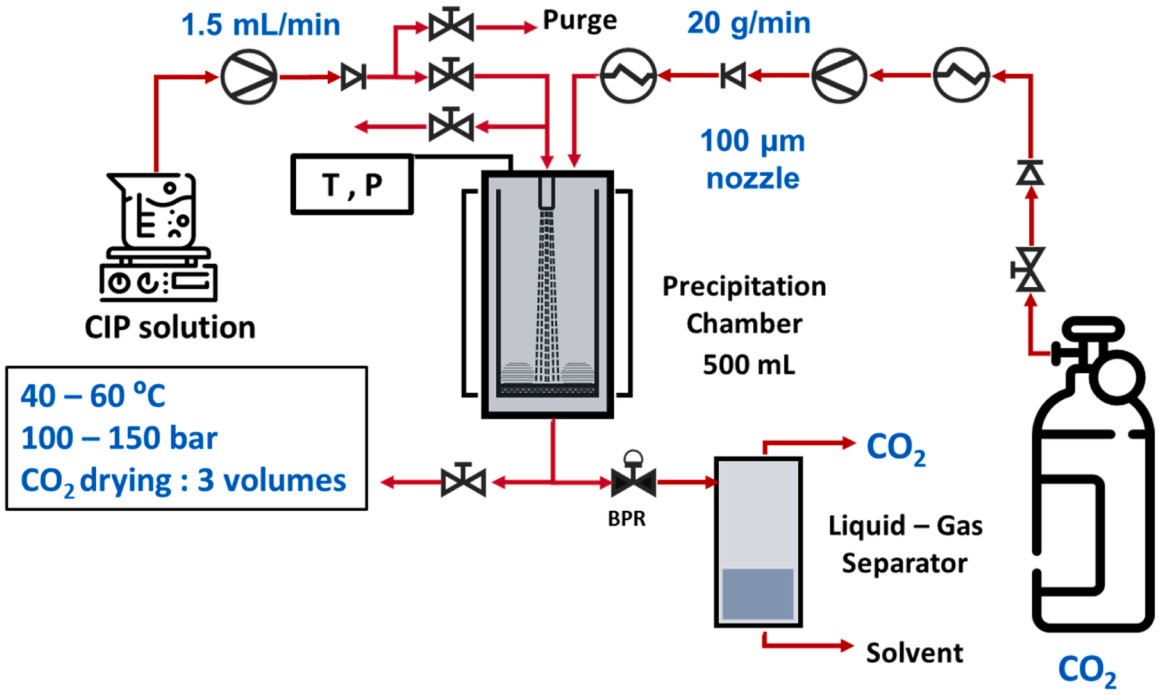

Fig. 2. Supercritical Anti-Solvent (SAS) equipment used in the micronization experiments, indicating the experimental conditions.

Quantification of the drug was performed by dissolving the samples in HCl 0.1 M and recording the absorbance of the solution at 277 nm. TGA of the samples were measured on an SDT- Q600 at a heating rate of 10 °C/min in N_2 flow using open aluminium crucibles. DSC was performed using two DSC Q-200 and DSC Q-10 apparatus from TA Instruments. The system was calibrated for both temperature and enthalpy using an indium standard. Samples were heated in N_2 flow from 10 to 250–350 °C, depending on the composition, at a heating rate of 10 °C/min. Nuclear Magnetic Resonance (NMR) of a solution of the ciprofloxacine base and the material precipitated by SAS in D_2O were recorded using a Bruker AVIIII 300 MHz BACS-60. A JEOL-6400 scanning electron microscope (SEM) working at 10 kV was used to characterize the microparticles. Samples were gold-coated prior to analysis. Particle size was determined from the SEM images using ImageJ free software.

2.4. Determination of the antimicrobial activity

Antibacterial activity was evaluated against s *Staphylococcus epidermidis*. The microorganism was recovered from the lyophilized state in which it was supplied by the CECT. Then it was inoculated in an Eppendorf with peptone water or nutritive broth for 2 h and scaled to a volume of 10 mL in a Falcon tube for 24 h. Afterwards, 2.5 mL were inoculated in a flask with 100 mL of culture medium nutritive broth in a bath at 37 °C provided with gentle lateral agitation for at least two days to achieve a high concentration of bacteria.

Cultures for experiments were prepared by transferring a sample from the culture in nutritive broth into tryptic soy broth. They were standardized to match 0.5 Mc Farland, a measurement of 0.10 (± 0.02) absorbance of the bacteria at a wavelength of 600 nm [41].

Stock solutions of CIP base, CIP·HCl and the SAS precipitates were prepared by dissolving the drugs in HCl 0.1 M solution to get the concentration of 5 mg/mL. After that, the compounds were diluted with tryptic soy broth to yield the required concentration. The concentrations of the samples tested were in the range of 0.10–0.40 µg/mL.

The solutions prepared with the antibiotics in the medium with the microorganism were incubated at 37 °C for 6, 12 and 24 h. The bacteria concentration was evaluated from the absorbance of the samples at a wavelength of 600 nm.

Tests were performed on the starting materials CIP base and CIP·HCl and in the samples micronized by SAS at 40 °C and 120 bar. Standard deviation of the measurements was lower than 5 %.

3. Result and discussion

Experiments were performed at a temperature between 40 and 60°C and a pressure between 100 and 150 bar. Table 1 summarizes the conditions of the tests performed using CIP in EtOH/AcH and CIP·HCl in MeOH and some of the characteristics of the precipitates. Experimental conditions were chosen above the mixture critical point of the systems CO_2 + EtOH and CO_2 + MeOH [31] as shown in Fig. 3. Experiments at 50 °C and 100 bar were performed at conditions very close to the critical line.

Both CIP and CIP·HCl were in the form of white crystals whilst the SAS precipitates gave yellowish fine powders. Micronization yield was between 40–86 % for CIP SAS and 70–76 % for CIP·HCl SAS. The lowest yields correspond to those conditions leading to the smallest particles and may be related to problems during the particle collection.

Some experiments were also performed by adding lactose, PVP K-30 and PVP K-10 polymers as excipients at 4:1, 2:1 and 1:1 drug: excipient mass ratios and gave yields between 62 % and 85 %.

A comprehensive characterization of the materials prepared is presented next. The crystal structure of the samples was studied by XRD. FTIR was used to determine the ionic form of the precipitates. Quantification of CIP in the precipitates was determined by UV–vis of the samples dissolved in HCl 0.1 M. Thermal analysis (TGA and DSC) was used to confirm the crystal structure of the precipitates and analyse the presence of water and solvent residues. Elemental analysis was used to determine the C to N ratio in the precipitates. These data along with the ^1H NMR of the sample dissolved in D_2O confirmed the presence of acetate in the CIP SAS samples. Finally, SEM analysis was used to determine the particle size and shape of the micronized materials.

3.1. XRD analysis

Fig. 4 compares the XRD patterns of the starting materials and the SAS precipitates obtained at 40 °C and 120 bar. XRD of all the samples

Table 1
Summary of micronization experiments of ciprofloxacine by SAS.

Drug form	Solvent	Excipient	Drug:excipient mass ratio (initial)	*T* (ºC)	*P* (bar)	Yield ± 10 (%)	Drug:excipient mass ratio by UV–vis ± 0.2*	Particle morphology	XRD/composition
CIP	AcH/ EtOH	-	-	40	100	60		Flat and elongated	Crystalline, unknown form/ CIP-acetate
				40	120	86		Flat and elongated	
				40	150	40		Rod-like	
				50	100	64		Flat and elongated	
				50	120	40		Flat and elongated	
				60	150	77		Flat and elongated	
CIP·HCl	MeOH	-	-	40	120	76		Rod-like	Crystalline structure, anhydrous AH1/CIP-chloride
				40	150	70		Rod-like	
				50	120	73		Rod-like/submicron irregular	
				50	150	70		Rod-like	
		PVP K-30	4	40	120	81	2.6	Flakes	
		lactose	4	40	120	65	2.7	Flakes	
		PVP K-10	4	40	120	85	2.9	Submicron irregular globular	
				40	150	68	2.8	Sheet-like	
			2	40	120	78	1.6	Sheet-like	
				40	150	62	1.6	Flakes + irregular round	
			1	40	120	62	1.1	Flakes	

* Ratios referred to CIP.

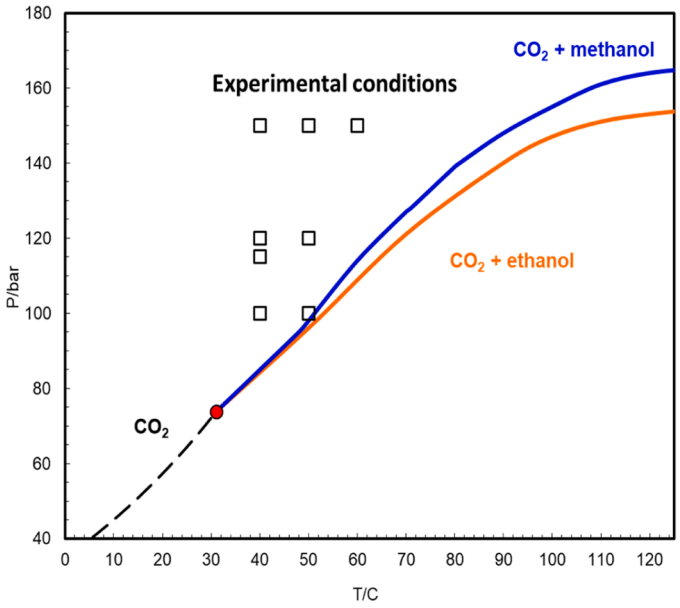

Fig. 3. PT projection of the critical lines for the systems CO_2 + EtOH and CO_2 + MeOH [31], showing the pressure and temperature conditions for the SAS experiments.

precipitated at the different conditions are provided as Supplementary material (Figs. S1–S3).

CIP and CIP SAS were crystalline materials but had different crystalline forms. The possibility of controlling the drug crystalline form upon SAS precipitation has been previously explored [42]. Thus it was not surprising to get a different crystalline form upon SAS micronization. The crystal structure of the SAS precipitates did not match any previously reported pattern.

The formation of ciprofloxacin salts with benzoic acid (BA), acetylsalicylic acid (ASA), p-coumaric acid (PCMA) and p-aminosalicylic acid (PASA) has been previously reported [43]. The possible formation of a similar salt containing acetic acid could be speculated according to the different XRD patterns obtained for the CIP SAS samples.

CIP·HCl XRD pattern matched the 00–061–1399 PDF file, corresponding to a crystal containing 1 HCl and 1.43 H_2O molecules per CIP molecule. CIP·HCl SAS was also crystalline but exhibited a different XRD pattern, which was also different to CIP SAS. All the CIP·HCl SAS samples showed the same crystal form although the relative intensity of some peaks was different.

Comparison of the XRD patterns with literature showed that CIP·HCl SAS samples corresponded to the anhydrous form of ciprofloxacin AH1 [44]. Thus during the micronization process, water was removed from the crystal structure. The dehydration of compounds upon SAS micronization has been previously reported for other systems [45,46]. Upon heating, AH1 form undergoes a solid-solid transition to a different anhydrous form, AH2. AH1 is reported to be unstable at relatively low relative humidity (23 %) and transforms into the hydrated CIP·HCl form in two weeks. Interestingly its solubility is much larger than that of CIP·HCl as well as the dissolution rate. [44] Nevertheless, the samples precipitated in this work were kept for months without showing change in their crystal structure.

XRD pattern of the sample precipitated using PVP K-10 at a 4:1 ratio was similar to that of the samples micronized without excipients and seemed to correspond to the AH1 anhydrous form. Similar results were obtained at a different drug:excipient ratios and using PVP K-30 (see Supplementary, Fig. S3). In contrast, the XRD pattern of the sample precipitated with lactose was different to the AH1 anhydrous form and also to those of pure hydrated lactose [47]. It is very interesting the large number of different crystal structures obtained in the micronization of this drug.

3.2. *FTIR analysis*

Figs. 5 and 6 compare the FTIR spectra of the starting materials CIP and CIP·HCl and the materials micronized by SAS at 40 ºC and 120 bar. As expected, CIP and CIP·HCl FTIR spectra were very different. The most important features are discussed next.

In the OH region, the FTIR spectrum of CIP·HCl (Fig. 5**b**) showed two strong bands at 3535 and a broad one at 3300 cm^{-1} associated with the O-H stretching vibration of the H_2O molecules in the hydrate and the carboxylic acid group, respectively. However, CIP·HCl SAS did not show the band at 3535 cm^{-1}, which confirmed the dehydration of the compound during the SAS micronization. The CIP SAS sample (Fig. 5**a**) showed a very weak but broad band in the O-H region. None of these bands were present in CIP, which indicated that the carboxylic acid group was deprotonated.

The other important difference in the spectra appeared in the

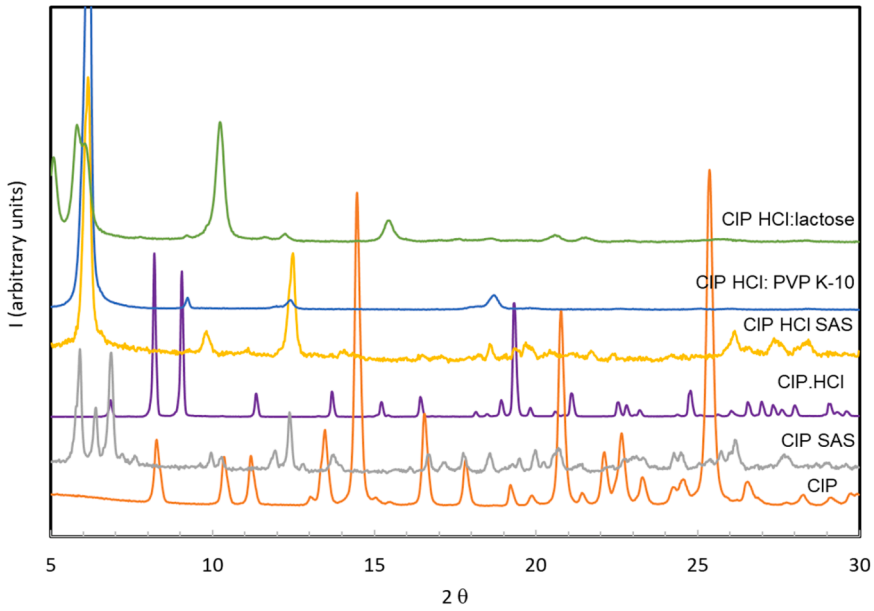

Fig. 4. XRD patterns of CIP and CIP·HCl starting materials and the materials precipitated by SAS at 40 °C and 120 bar.

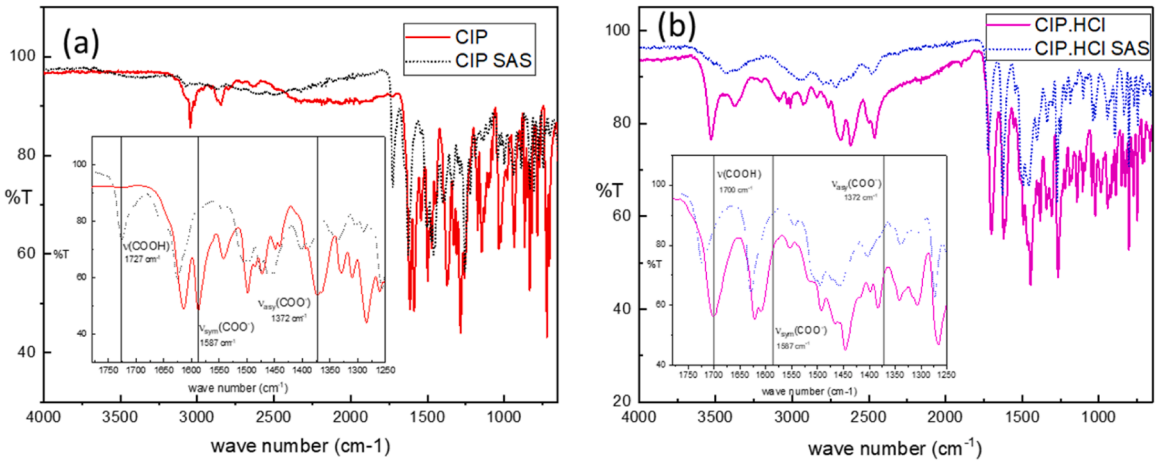

Fig. 5. FTIR spectra of: (a) CIP and CIP SAS, (b) CIP·HCl and CIP·HCl SAS. SAS samples precipitated at 40 °C and 120 bar. Insets in both figures show an enlargement of the carbonyl region.

carbonyl region around 1700 cm^{-1}. CIP contains a carboxylic acid group (pa_1 = 5.90) and an amino group (pKa_2 = 8.89) which present a different form depending on the pH [48] (Fig. 7). At pH below 5.90, CIP is in the cationic form and the carboxylic and the amino groups are both protonated. Between 5.90 and 8.89, the molecule is in the zwitterionic form and the carboxylic acid group is deprotonated whilst the amino group is protonated. At pH above 8.89, CIP is in the anionic form and only the carboxylic acid group is deprotonated. The prevalence of each form can be easily followed by vibrational spectroscopy of the carbonyl region. At acidic pH, the protonated carboxylic acid group gives a unique strong signal at a wave number close to 1700 cm^{-1}, whilst in the zwitterionic form, the COO^- group shows two strong bands at 1587 and 1372 cm^{-1} associated with the antisymmetric and symmetric stretching bands in COO^-.

Thus, analysis of the carbonyl region in Fig. 5 revealed that CIP base was in the zwitterion form, whilst CIP·HCl and any of the SAS precipitates from CIP and CIP·HCl appeared in the protonated form corresponding to a cationic form. The position of the C═O band in all the SAS precipitates was very similar and appeared at a slightly higher frequency than in CIP·HCl (1727 cm^{-1}). FTIR of CIP·SAS also showed a shoulder at 1650 cm^{-1}. For both CIP and CIP·HCl, FTIR spectra of the SAS precipitates did not change with pressure and temperature conditions.

FTIR of the samples precipitated with PVP K-10, and lactose at 40 °C and 120 bar are compared in Fig. 6 with the spectra of CIP·HCl SAS and the pure excipients. Spectra of the composite materials were very similar to that of CIP·HCl SAS alone at the same conditions, except for the addition of a few bands associated to the excipients. Analysis of the carbonyl region (inset in the Figures) confirmed that ciprofloxacin in CIP·HCl: PVP and CIP·HCl: lactose were in the protonated form. Furthermore, FTIR of any of the CIP·HCl SAS precipitates did not show the strong band at 3535 cm^{-1} present in the CIP·HCl hydrate, confirming the loss of hydration water during the SAS micronization. Strong interactions of the drug and the excipients were not evidenced by FTIR.

Summarising, FTIR analysis indicated that during SAS micronization there were changes in the structure of the drug. Hydrated CIP·HCl lost water during the SAS process leading to the anhydrous protonated ciprofloxacin salt ($COOH–R–NH_2^+Cl^-$). Similarly, the SAS micronization of the CIP solution containing acetic acid seemed to render the protonated ciprofloxacin form, possibly as an acetate ($COOH–R–NH_2^+CH_3COO^-$) instead of the zwitterion ($COO^-–R–NH_2^+$). The higher acidity of acetic

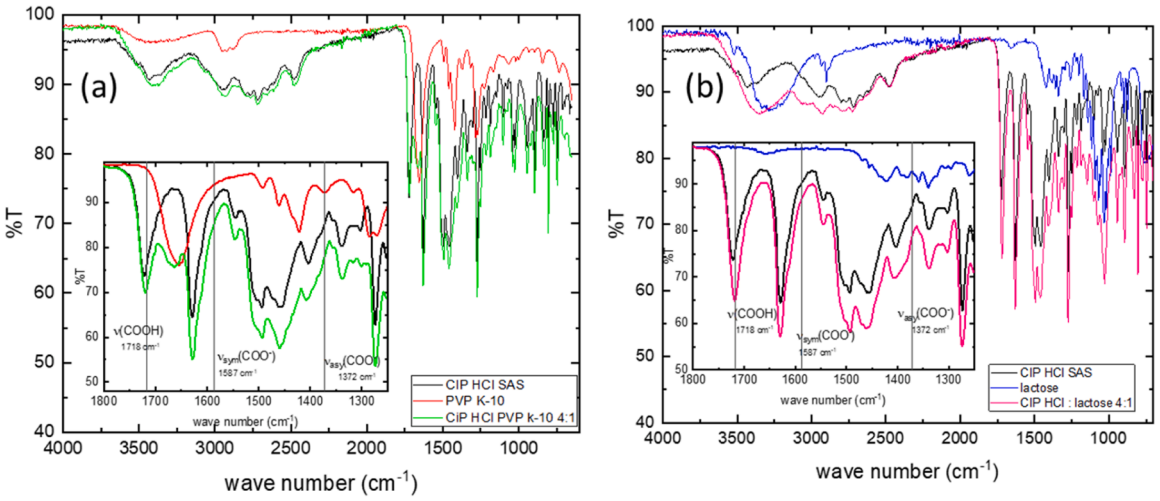

Fig. 6. FTIR spectra of: (a) CIP·HCl SAS, PVP K-10 and CIP·HCl:PVP K-10 4:1 SAS (b) CIP·HCl SAS, lactose and CIP·HCl:lactose 4:1 SAS. Insets in both figures show an enlargement of the carbonyl region.

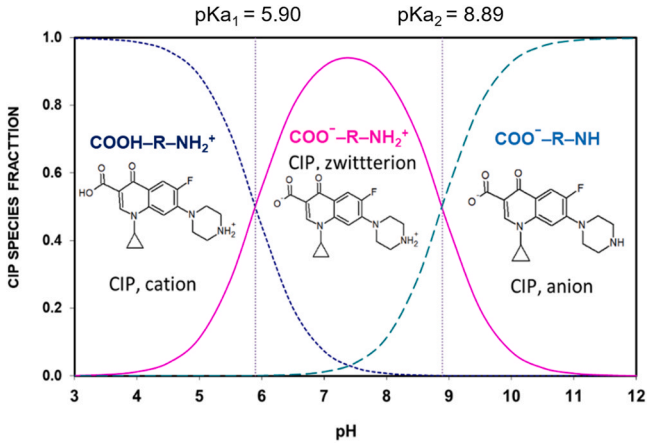

Fig. 7. Structure of ciprofloxacin (CIP) as a function of pH (adapted from [48]).

acid ($pKa_1 = 4.76$ [49]) in comparison to the carboxylic acid group in ciprofloxacin ($pKa_1 = 5.9 = 5.9$ [48]) would favour the formation of this salt.

The CIP zwitterion had very low solubility in water [29]. In contrast, CIP·HCl hydrate was in the protonated form which was much more soluble in water (30 mg/mL) [30]. The solubility of the anhydrous CIP·HCl SAS form AH1 was higher than that of the hydrochloride [44]. CIP·SAS would be more water soluble than CIP but less than CIP·HCl and CIP·HCl SAS. The different solubility of the precipitates could be used to control the residence time of the drug in the lungs.

3.3. UV–vis analysis

UV–vis absorption spectra of CIP, CIP·HCl and the different SAS samples were recorded in HCl 0.1 M. The amount of CIP base present in the samples was determined from the absorbance of the drug at 277 nm. CIP SAS samples gave drug percentages in the precipitates between 81 % and 87 %, depending on temperature and pressure conditions, confirming the presence of other molecules in the precipitates. The higher the temperature and pressure conditions, the higher the percentage of the drug in the precipitate. CIP·HCl SAS samples yielded drug contents equal to 90 %.

Assuming that CIP SAS is in the form of a ciprofloxacin acetate salt, the calculated percentage of CIP in the sample would be equal to 84.6 %. This value was quite similar to those measured by UV–vis in the CIP SAS precipitates. The calculated percentage of CIP in CIP·HCl starting material (84.2 %) also agreed well with the expected percentage considering 1.43 mol of H_2O and 1 mol of HCl in the structure [44]. The percentage of CIP in the CIP HCl SAS samples also confirmed the loss of water during the SAS micronization.

The drug content in the samples micronized with PVP K-30, PVP K-10 and lactose was also determined in the same way. The theoretical drug to excipient mass ratios referred to CIP instead of CIP·HCl were 3.7:1, 1.9:1 and 0.9:1. The molar masses of CIP HCl hydrate, CIP·HCl anhydrous form and CIP used in the calculations were 393.54, 367.81 and 331.35 g/mol, respectively. The analysis showed lower incorporation of the drug in comparison to the theoretical values, with drug to excipient mass ratios close to 3:1, 1.6:1 and 1:1. The lower drug content may be related with the uncomplete precipitation of the pure drug (yields 70–80 %, Table 1).

3.4. TGA and DSC analysis

Thermal analysis of the samples was performed by TGA and DSC. Fig. 8 compares TGA of CIP and some of the CIP SAS precipitates at different temperature and pressure conditions. CIP started to decompose at ca. 300 °C under N_2 and decomposed in two steps. In contrast, SAS samples started to decompose at a slightly lower temperature. Some of the SAS samples also showed an appreciable weight loss from 100 to 175 °C, up to 10 % mass at 40 °C and 120 bar. This weight loss decreased strongly at high temperatures and pressure. The residue of the samples after heating in N_2 was between 20 % and 30 % (w/w).

DSC analysis of CIP and the CIP SAS samples are shown in Fig. 9. DSC of SAS samples showed a broad endotherm at temperatures ranging from 25 to 125 °C. This was followed by another small endotherm from 125 to 175 °C. TGA analysis of SAS samples also showed an appreciable mass loss below 175 °C (Fig. 8). DSC of the starting CIP drug did not show any thermal transition in this range. Thus, these events may be related to the solvent mixture (AcH/EtOH). The event below 125 °C would correspond to the evaporation of ethanol or most likely water adsorbed on the precipitate whilst the endotherm between 125 and 175 °C may be due to the evaporation of acetic acid adsorbed on the CIP SAS precipitates. This second endotherm disappeared almost at the highest temperature and pressure (60 °C, 150 bar) whilst the first one did not change much with precipitation conditions.

At higher temperatures, DSC analysis of CIP showed an endothermic peak due to the melting of the drug at an onset temperature of 271.9 °C. This was followed by an exotherm due to the recrystallization of CIP, possibly to a different solid phase, followed by other exotherms. The

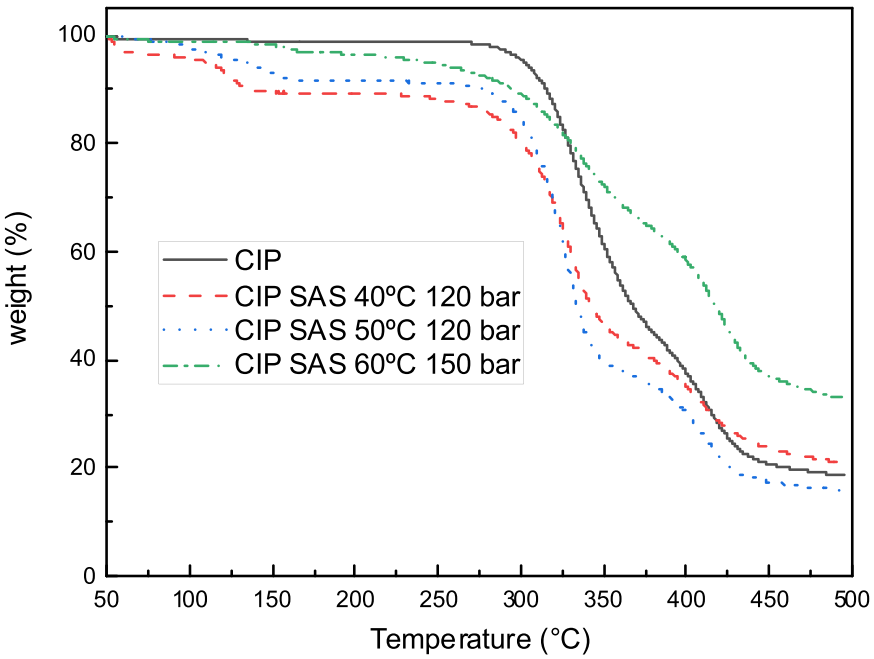

Fig. 8. TGA analysis of CIP and CIP SAS precipitated at different pressure and temperature conditions.

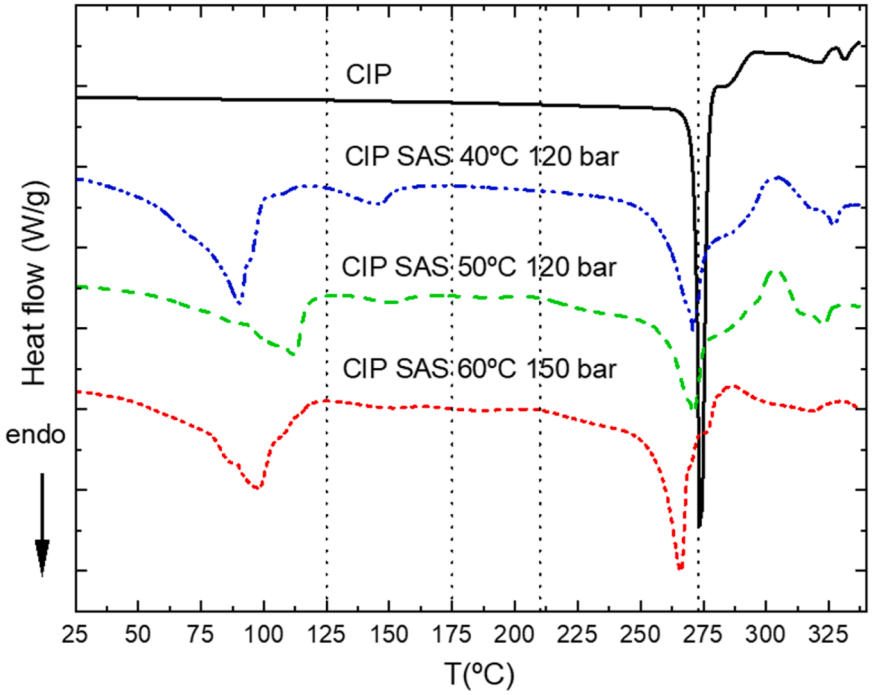

Fig. 9. DSC analysis of CIP and the CIP SAS samples precipitated at different pressure and temperature conditions.

decomposition of CIP started at 300 ºC, so that no information could be extracted from this temperature. In the CIP SAS samples, the endotherm peak associated with the drug melting was broader and was shifted to a lower temperature (270–266 ºC), which may be related to the different crystal structure (XRD pattern).

The incorporation of acetic acid into the CIP SAS precipitates was confirmed by elemental analysis (see Supplementary data Table S1). SAS precipitates showed higher C:N and lower C:O molar ratios than the expected ones. The presence of acetic acid in the CIP SAS precipitates was further confirmed by ^{1}H NMR of the sample dissolved in D_2O.

We speculated the possible formation of a ciprofloxacin salt with acetic acid, in agreement with XRD, FTIR and UV–vis analysis of the CIP SAS samples. However, no definite conclusion could be extracted as the change in the melting point of the CIP SAS samples in comparison to the starting material was very low in comparison to previous reports on salt formation [43]. A small amount of the acid was also adsorbed on the precipitate at the lower temperature and pressure conditions. This should not necessarily be detrimental, as the combined use of acetic acid and ciprofloxacin has proved effective in the treatment of chronic suppurative otitis media. [50]

Similarly, samples precipitated using CIP·HCl were also studied by TGA and DSC. TGA of the commercial CIP·HCl in Fig. 10 showed a mass

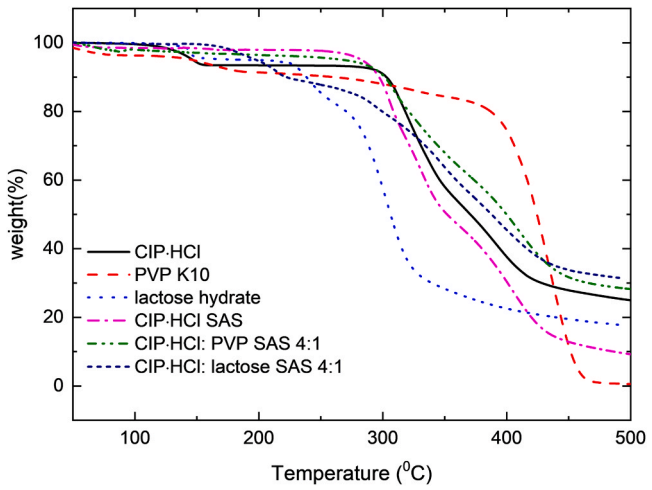

Fig. 10. TGA analysis of CIP·HCl, PVP K-10, lactose and SAS samples precipitated at 40 °C and 120 bar: CIP·HCl, CIP·HCl:PVP K-10 4:1, CIP·HCl:lactose 4:1.

loss of ca. 6–7 % from 100 to 160 °C which, according to previous reports, corresponded to the loss of 1.43 mol of hydration water from the structure [44]. Decomposition under N_2 atmosphere only started at ca. 300 °C and took place in two steps. The decomposition was not complete, leaving a black foam residue larger than 20 %(w/w).

In contrast, the TGA of the CIP·HCl SAS sample precipitated at 40 °C and 120 bar showed a small weight loss below 75 °C, attributed to adsorbed solvent or water, without any significant mass loss in the 100–160 °C range. Thus TGA confirmed that CIP·HCl SAS, although might contain a small amount of adsorbed water, was in a dehydrated form in agreement with the XRD findings [44]. Decomposition of the CIP·HCl SAS started at a slightly lower temperature than the commercial material, leaving a smaller residue.

TGA of PVP showed the loss of water below 100 °C, followed by two small mass losses from 150 to 200 °C and 200 to 325 °C. This suggested the presence of impurities (lower molecular weight polymers or residual monomers) in the commercial polymer. Then decomposition started at 400 °C. TGA of the CIP·HCl: PVP K-10 sample resembled the TGA of SAS CIP.HCl and took place in two steps. However, the second decomposition step shifted to higher temperatures. Curiously, the impurities present in PVP observed at low temperature disappeared during the SAS precipitation process.

TGA of lactose showed a first mass loss at ca. 150 °C assigned to the loss of hydration water of the excipient. Then lactose decomposed in two steps at ca. 225 and 300 °C. In contrast, the CIP·HCl:lactose SAS precipitate presented an appreciable mass loss between 175 and 220 °C that could be ascribed to water. The higher temperature of this event in comparison to lactose or CIP·HCl indicated a different environment of water in this precipitate. Then the composite decomposed from 275 to 450°C in three continuous steps, the first one coincident with lactose and the other two similar to the drug but shifted to higher temperatures.

DSC analysis of all these samples is presented in Fig. 11. DSC of commercial CIP·HCl showed a sharp endothermic peak with an onset temperature of 145.1 °C, possibly due to the dehydration of the drug, followed by a small shoulder at a higher temperature. In contrast to previous publications [44], the phase transformation of the expected form after dehydration, AH1 to AH2, was not seen. DSC of pure PVP in the same range showed a broad endotherm between °C, possibly related to water and impurities as observed by TGA.

DSC of the CIP·HCl SAS samples did not show the endothermic dehydration peak of the drug confirming that the precipitates are in the AH1 anhydrous form (XRD). SAS samples showed two broad endothermic peaks between 25 and 125 °C which could be associated with the loss of a small amount of adsorbed solvent and water, respectively, followed by an exothermic peak between 175 and 225 °C, due to the recrystallization of the drug to AH2 form [44]. The first peak due to the solvent, decreased as the pressure and temperature increased, becoming very weak at 50 °C and 150 bar. The second one, due to adsorbed water, decreased at high temperatures but increased slightly with pressure. The recrystallization of CIP·HCl SAS took place at lower temperatures than those found in the different CIP·HCl:PVP K-10 SAS samples due to the presence of the polymer. In these samples, the anhydrous form decomposed below 300 °C without melting. Similar thermograms were obtained for the 4:1 and 2:1 CIP·HCl:PVP K-10 composites. Thermograms of the SAS precipitates obtained at 40 °C ad 120 and 150 bar were also very similar.

DSC of lactose hydrate and the CIP·HCl:lactose 4:1 sample

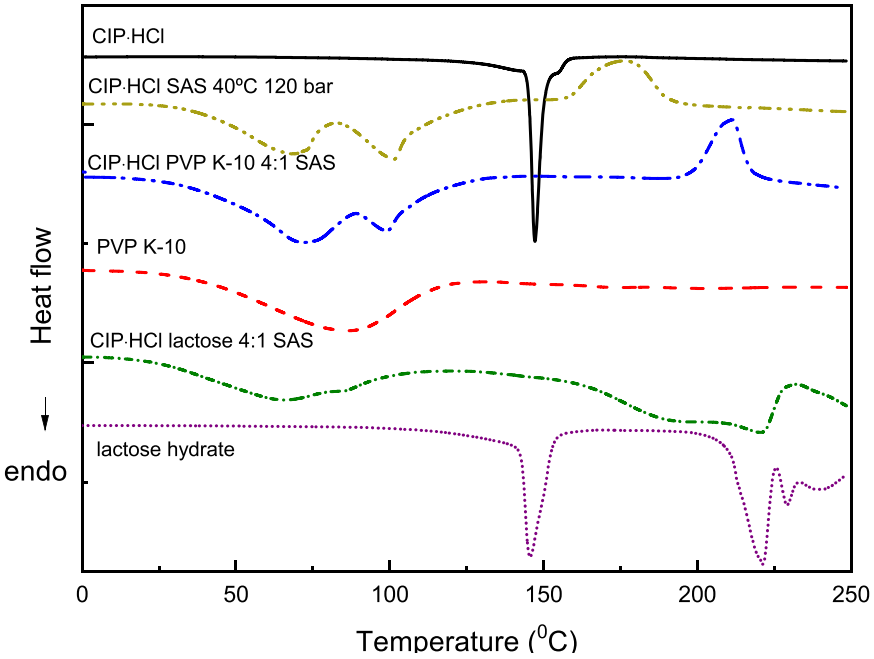

Fig. 11. DSC analysis of CIP·HCl, PVP K-10, lactose and SAS samples precipitated at 40 °C and 120 bar: CIP·HCl, CIP·HCl:PVP K-10 4:1, CIP·HCl:lactose 4:1.

precipitated by SAS at 40 ºC and 120 bars are also shown in Fig. 14. Pure lactose showed an endotherm at onset temperature equal to 142.6 ºC which corresponded to the loss of water in the structure. Then, the sample decomposed from 210 ºC. The CIP·HCl:lactose 4:1 SAS precipitate showed two broad peaks below 110 ºC due to the solvent and water evaporation. Another two broad peaks appeared in the thermogram between 160 and 230 ºC. The second peak was related to the decomposition of the excipient. Recrystallization of the drug with lactose from AH1 to AH2 was not observed.

3.5. SEM analysis

SEM images of the drug in the different ciprofloxacin forms before micronization are shown in Fig. 12. Commercial CIP base was heterogeneous in size, showing large particles more than 10 μm long, along with much smaller particles $\leq$ 1 μm. In contrast, the CIP·HCl starting material was formed by much larger particles, up to 100 μm, with a more regular morphology.

Fig. 13 shows SEM images of CIP precipitated by SAS. The precipitated drug exhibited an acicular morphology which varied from needle-like or rod-like to flat and elongated particles depending on the temperature and pressure conditions. Particles were 0.2–0.9 μm wide × 1–4 μm long showing the successful micronization of the drug. Small variations of size were observed with temperature and pressure. At constant temperature, the particles became thinner as the pressure rised, and their length to width ratio increased. At the lowest pressure, particles appeared flattened. At constant pressure, the thickness increased slightly with temperature. At 50 ºC and 100 bar, a slightly twisted material was observed. This could be related to the proximity of the experimental conditions to the CO_2 + ethanol mixture critical point (Fig. 3) which would lead to some agglomeration [51].

Similar results were obtained from the precipitation of CIP·HCl. Fig. 14 showed needle-like elongated particles comparable in size to the previous ones. Variations with pressure and temperature were however different from those found in the precipitation of CIP. At constant temperature, the length-to-width ratio seemed to decrease as the pressure increased and particles became shorter at the higher pressure. At constant pressure, particles became shorter and/or thinner as the temperature increased. At 50 ºC and 120 bar a mixture of long and very short rods/round particles of size close to 200 nm were observed. The different trend with pressure and temperature was not surprising considering the compositional and structural differences between the CIP SAS and CIP·HCl SAS precipitates (CIP·HCl SAS is in the AH1 dehydrated form).

Although CIP and CIP·HCl drugs were successfully micronized, particles showed in most cases an acicular morphology that may not be adequate for pulmonary delivery. Although acicular particles could present better aerosol performance than spherical ones, the uniformity in the mixture composition could be compromised when they are mixed with different carriers/excipients [52]. Furthermore, it has been reported that particles with this morphology may stimulate the pro-inflammatory response in the organism [53,54]. Thus, aiming to change their morphology, CIP·HCl mixed with different excipients was micronized. Fig. 15 shows images of the precipitates.

CIP.HCl combined with lactose or PVP K-30 and K-10 precipitated at most conditions in the form of flakes. At 40 ºC and 120 bar and a 4:1 drug to polymer ratio, precipitation yield was slightly lower with lactose (65 %) in comparison to PVP (> 80 %). The addition of PVP K-10 led to a drastic change in morphology and size and SEM images showed submicron irregular globular particles at a 4:1 drug to polymer ratio. Increasing the amount of polymer led to precipitates with a sheet-like morphology (2:1) an flakes (1:1). At 40 ºC and 150 bar at the 4:1 and 2:1 drug:polymer ratios, particles became less homogeneous and consisted of a mixture of small irregular particles and flakes. The pressure seemed to promote aggregation. The flake and sheet-like morphology of the precipitates could be beneficial for drug delivery to the lungs. These results highlight the important role of the excipient in the micronization process by SAS.

3.6. Antibacterial activity

The antibacterial activity of some of the samples was evaluated against *Staphylococcus epidermidis* and compared to a standard Ciprofloxacin base solution dissolved in 0.1 M HCl. This gram-positive bacterium plays a significant role in the microbiota of human skin and mucous membranes. Under certain circumstances, this bacterium can become an opportunistic pathogen causing serious blood-borne infections, especially in immunocompromised individuals or those with implants.

Absorbance in the presence of the bacteria was measured at different drug concentrations and followed with time. Lower absorbances (higher antibacterial activity) were obtained for the 0.3 μg/mL drug solution which was selected as the optimal concentration for further experiments.

Fig. 16 shows the % bacterial growth estimated as the percentage ratio between the absorbance of the bacteria containing 0.3 μg/mL drug and the absorbance of the control (without drug) at different times. All the samples were active against *Staphylococcus epidermidis* and reduced the bacterial growth. For each sample, the bacterial growth increased with time which indicated that the drug at this concentration would need to be replenished with time. A comparison of the bacterial growth for the different samples at 6 hours revealed that the most active form

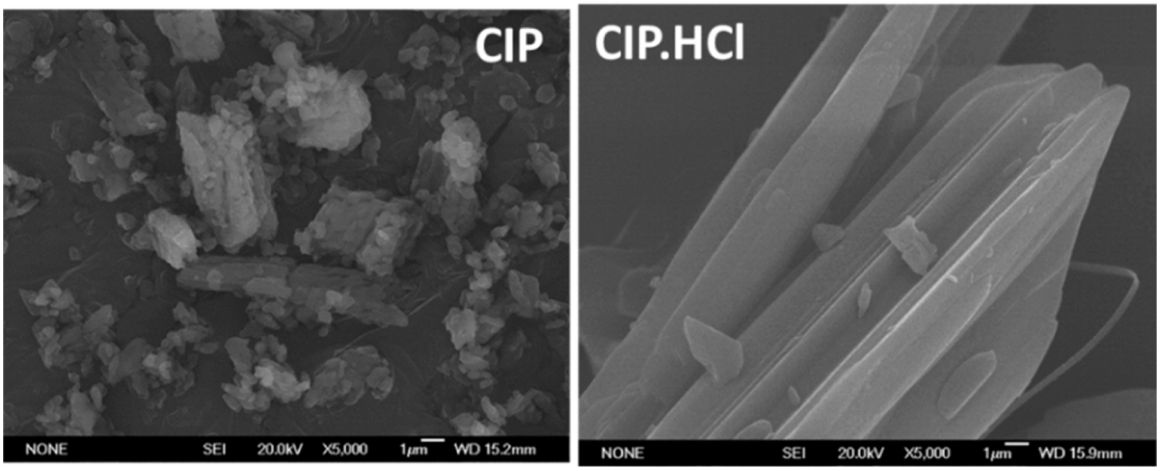

Fig. 12. SEM images of CIP and CIP·HCl starting materials.

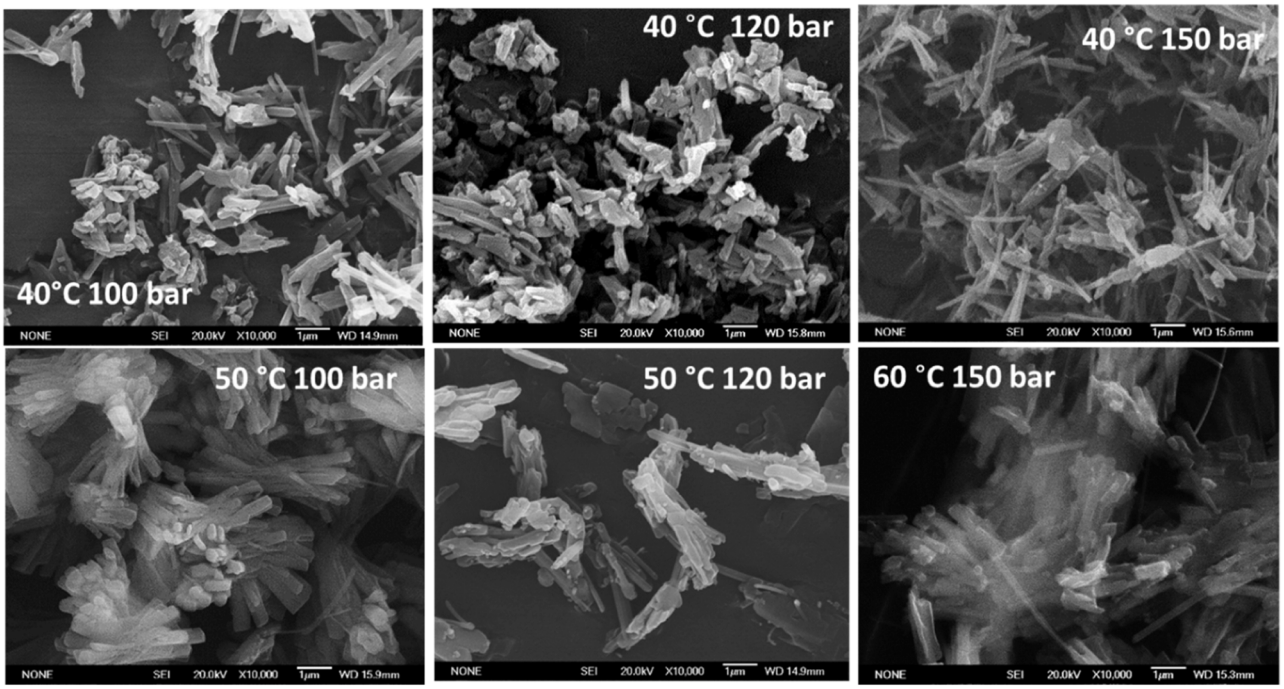

Fig. 13. SEM images of CIP samples precipitated by SAS at different pressure and temperature conditions.

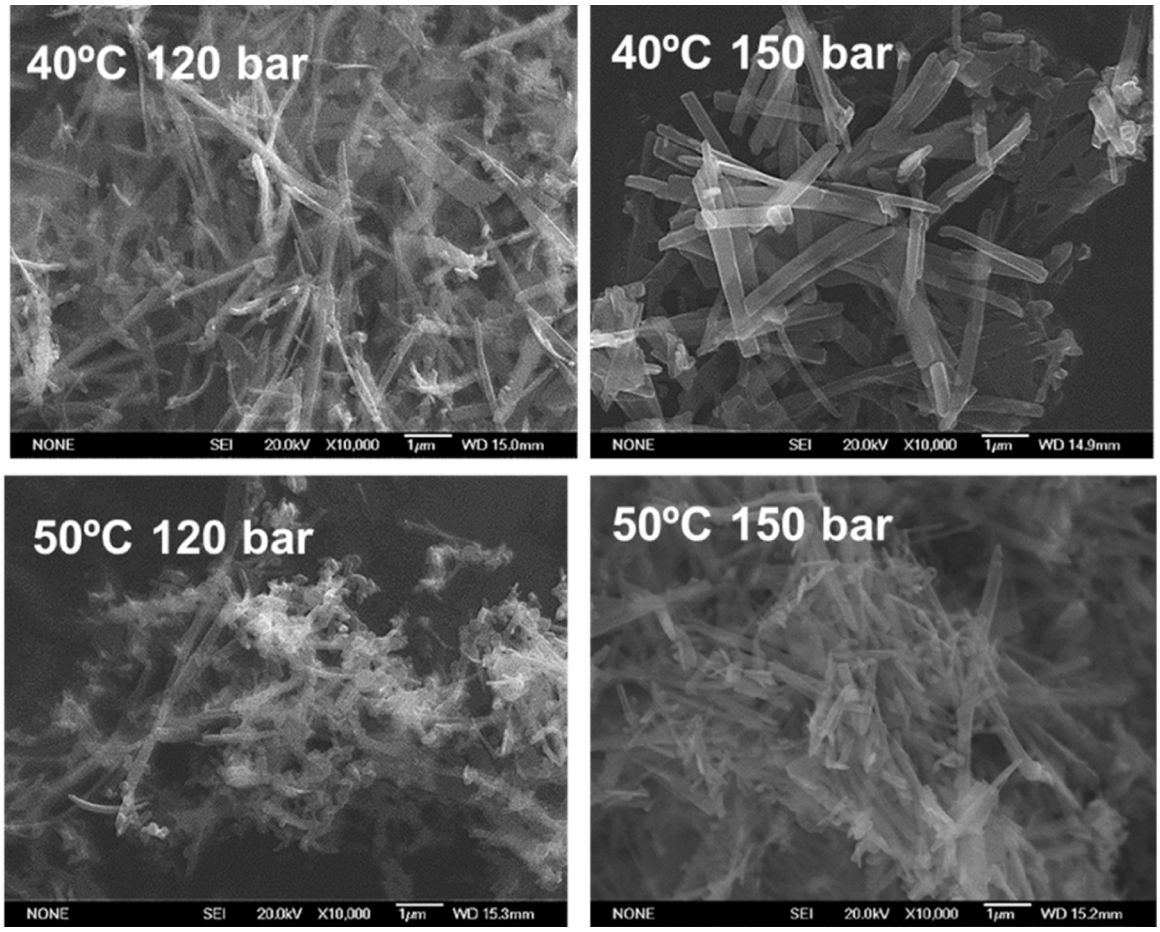

Fig. 14. SEM images of CIP·HCl samples precipitate by SAS at different pressure and temperature conditions.

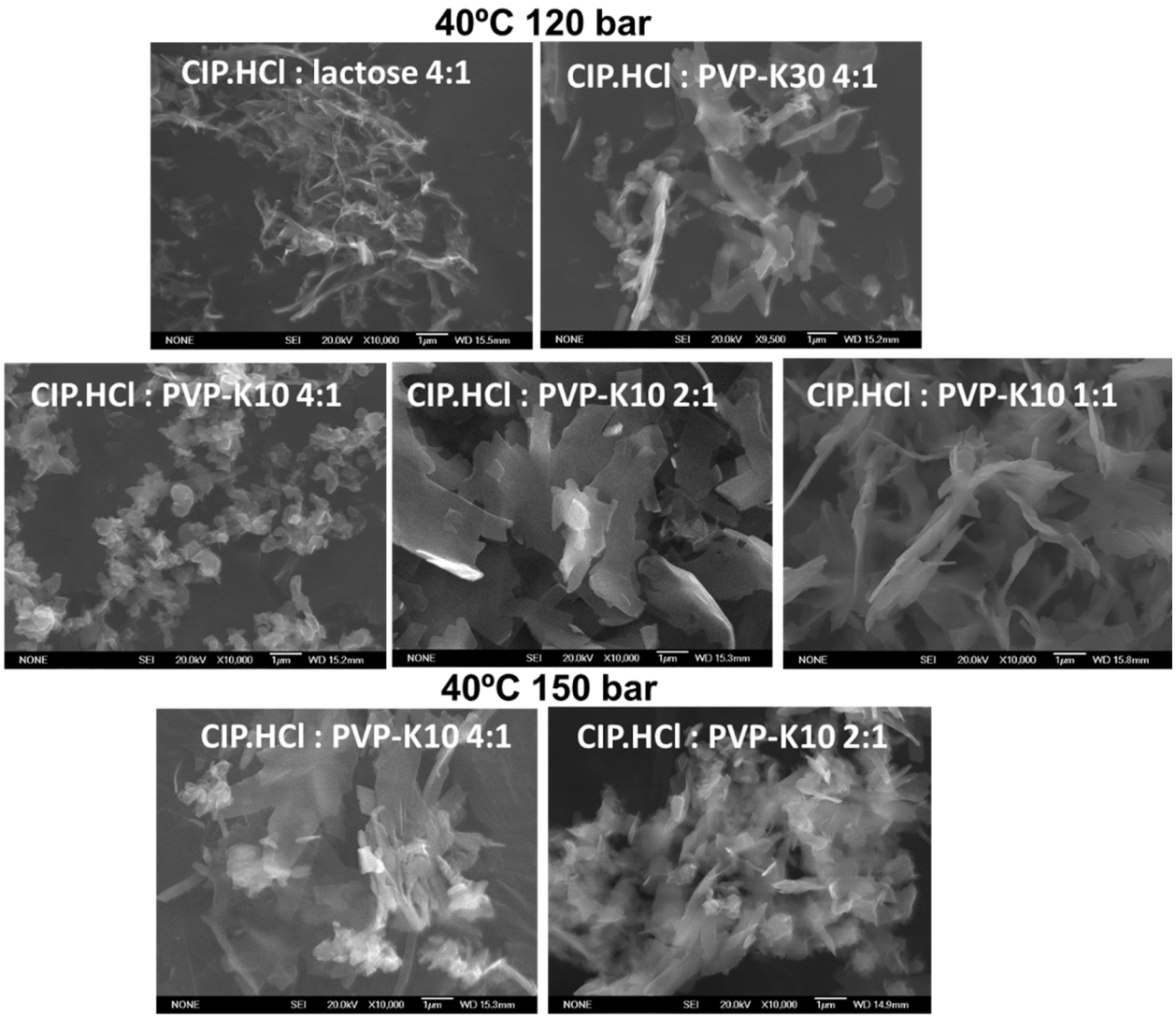

Fig. 15. SEM images of CIP·HCl samples with several excipients precipitate by SAS and different drug to excipient ratios at 40 ºC and 120 and 150 bar.

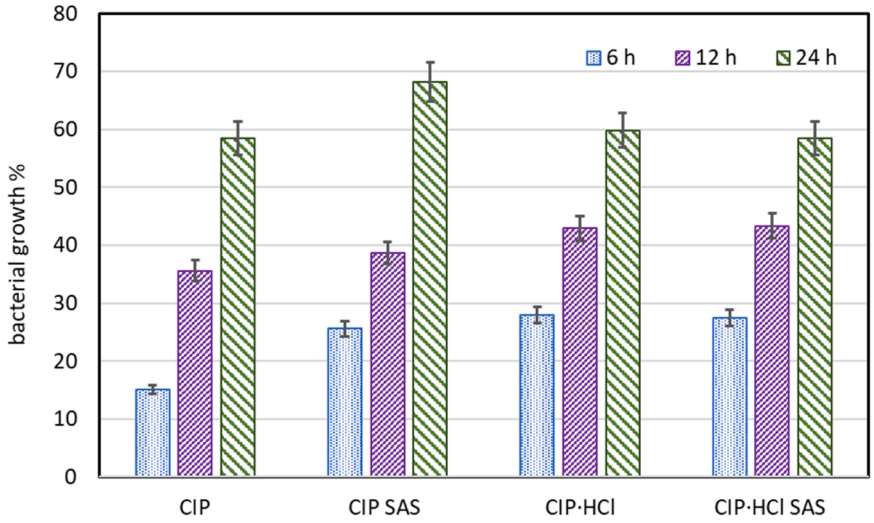

Fig. 16. Bacterial growth at increasing times for 0.3 μg/mL ciprofloxacine drug solutions. SAS samples were micronized at 40 ºC and 120 bar.

was CIP presenting the lowest bacterial growth. Then samples CIP SAS, CIP·HCl and CIP·HCl SAS showed a very similar behaviour. These differences could be related to the lower ciprofloxacin content in the different samples. CIP SAS seemed to correspond to the acetate form (85 % CIP), CIP·HCl contained HCl and H_2O (84 % CIP) and CIP·HCl SAS contained HCl (90 % CIP). Differences between the activity of the CIP and CIP·HCl and their SAS precipitates decreased after 12 and 24 h.

Different antimicrobial activity were previously reported for different ciprofloxacin salts [41]. The antimicrobial activity of ciprofloxacin increased with the lipophilic character of the molecule, which would allow it to easily cross the cell membranes of the microorganisms. It also depended on the ions present in the molecule, which would allow it to interact with some specific targets inside the bacterial cell.

4. Conclusions

Ciprofloxacin drug was successfully micronized using the SAS technique between 40–60 ºC and 100–150 bar. Two different commercial forms were used: ciprofloxacin base (CIP) and ciprofloxacin hydrochloride (CIP·HCl). FTIR analysis showed that CIP was in the zwitterion form (deprotonated carboxylic acid group and protonated amine group), which is scarcely soluble in water and ethanol. The addition of acetic acid was performed to solubilise the drug in EtOH. Hydrated CIP·HCl was however in the cationic form (protonated carboxylic acid and amine groups). This form is more soluble in water and could be dissolved in MeOH. During the SAS micronization of the CIP/AcH/EtOH and CIP·HCl/MeOH solutions, there were changes in the composition of the drug which led to different crystalline forms (XRD). CIP SAS incorporated acetic acid forming possibly an acetate salt with the protonated amine group (XRD pattern did not match any of the reported ones), whilst CIP·HCl lost water leading to the anhydrous form AH1 (according to XRD and DSC). The formation of new salts could be used to modify the physicochemical properties of ciprofloxacine. CIP SAS samples also incorporated a small amount of EtOH, water and possibly acetic acid. Similarly, CIP·HCl SAS samples also showed the presence of small amounts of water and methanol.

SAS micronization of CIP and CIP·HCl led to particles 0.2–0.9 μm wide × 1–4 μm long. The precipitates exhibited an acicular morphology with rod-like or flat and elongated particles. Although the length of the particles was right for a pulmonary device, the morphology may pose some problems. Aiming to modify the morphology of the precipitates, CIP·HCl was micronized along with some common excipients: lactose, PVP K-10 and PVP K-30 at different drug to excipient mass ratios. Indeed, the addition of excipients did not modify the crystalline form of the CIP·HCl SAS precipitates but changed their morphology leading to flakes, sheets or globular particles. The flake and sheet-like morphology may be less invasive to the lungs and at the same time may prevent powder agglomeration during inhalation improving the aerosol performance of these composites. On the other hand, CIP·HCl:PVP K-10 1:4 SAS sample was formed by submicron irregular globular particles that could be used for an oral formulation. The antibacterial efficacy of the different samples was also assessed for *Staphylococcus epidermidis* confirming that the SAS precipitates kept their antibacterial activity.

Ciprofloxacin turned out to be a very complex molecule to micronize. The high reactivity of the carboxylic and amine groups favoured its interaction with the solvent and additives in the system and challenged the micronization of the drug leading to some new crystal forms.

Although some solvent residues were incorporated into the samples at the conditions of this study, according to the United States Pharmacopeia (USP) ethanol and acetic acid are class 3 solvents with low toxic potential to humans so a limit of 5000 ppm or 0.5 % would be acceptable without justification. Higher amounts may also be acceptable providing they are realistic with manufacturing capability and good manufacturing practice (GMP). Methanol is a class 2 solvent that should be limited to 3000 ppm or 0.3 % in drug formulations. Thus longer washing times would be required to remove the solvent residues from the SAS samples.

This work demonstrates how the drug starting form, the solvents, additives and excipients, in addition to the temperature and pressure conditions, play an important role in the SAS micronization process and allow controlling the morphology of the precipitates.

CRediT authorship contribution statement

Fouad Zahran: Validation, Investigation, **Pablo Marzal**: Investigation, **Helga K. Ruiz**: Investigation, **Eduardo Pérez**: Writing – review & editing, Investigation, **Lourdes Calvo**: Writing – review & editing, Supervision, Resources, Project administration, Funding acquisition, **Albertina Cabañas**: Writing – original draft, Visualization, Supervision, Resources, Project administration, Methodology, Funding acquisition, Formal analysis, Conceptualization.

Declaration of Competing Interest

"There are no conflicts to declare".

Data availability

Data will be made available on request.

Acknowledgements

This work was funded by the Spanish Ministry of Science, Innovation and Universities (MICIU), through research projects RTI2018-097230-B-100 and PID2022-137847OB-100. P.M. thanks the Madrid Regional Government (CAM) for funding through a Research Contract. F.Z. thanks the Ministry of Higher Education of Egypt for funding his research stay at UCM. We thank Prof. E. Enciso at UCM for the use of FTIR facilities. We acknowledge the Centers of Scientific Instrumentation at UCM (X-ray diffraction) and ICTS National Microscopy Center and their staff, for use of the technical facilities.

Appendix A. Supporting information

Supplementary data associated with this article can be found in the online version at doi:10.1016/j.supflu.2024.106413.

References

[1] G.A. Shazly, Ciprofloxacin controlled-solid lipid nanoparticles: characterization, in vitro release, and antibacterial activity assessment, BioMed Res. Int. 2017 (2017) 2120734, https://doi.org/10.1155/2017/2120734.
[2] ⟨https://go.drugbank.com/drugs/DB00537⟩, (Accessed 16 Septemeber 2024).
[3] S. Chono, T. Tanino, T. Seki, K. Morimoto, Influence of particle size on drug delivery to rat alveolar macrophages following pulmonary administration of ciprofloxacin incorporated into liposomes, J. Drug Target 14 (2006) 557–566, https://doi.org/10.1080/10611860600834375.
[4] R. Wilson, T. Welte, E. Polverino, A. De Soyza, H. Greville, A. O'Donnell, J. Alder, P. Reimnitz, B. Hampel, Ciprofloxacin dry powder for inhalation in non-cystic fibrosis bronchiectasis: a phase II randomised study, Eur. Respir. J. 41 (2013) 1107–1115, https://doi.org/10.1183/09031936.00071312.
[5] ⟨https://cima.aemps.es/cima/publico/lista.html⟩, (Accessed 16 Septemeber 2024).
[6] S.N. Muchohi, N. Thuo, J. Karisa, A. Muturi, G.O. Kokwaro, K. Maitland, Determination of ciprofloxacin in human plasma using high-performance liquid chromatography coupled with fluorescence detection: application to a population pharmacokinetics study in children with severe malnutrition, J. Chromatogr. B Anal. Technol. Biomed. Life Sci. 879 (2011) 146–152, https://doi.org/10.1016/j.jchromb.2010.11.032.
[7] C. National Center for Biotechnology Information, PubChem Annotation Record for, Source: Hazardous Substances Data Bank (HSDB), 2023. Retrieved November 24, 2023 from ⟨https://pubchem.ncbi.nlm.nih.gov⟩.
[8] I. d'Angelo, C. Conte, M.I. La Rotonda, A. Miro, F. Quaglia, F. Ungaro, Improving the efficacy of inhaled drugs in cystic fibrosis: challenges and emerging drug delivery strategies, Adv. Drug Deliv. Rev. 75 (2014) 92–111, https://doi.org/10.1016/j.addr.2014.05.008.
[9] J. Sousa, G. Alves, P. Oliveira, A. Fortuna, A. Falcão, Intranasal delivery of ciprofloxacin to rats: a topical approach using a thermoreversible in situ gel, Eur. J. Pharm. Sci. 97 (2017) 30–37, https://doi.org/10.1016/j.ejps.2016.10.033.

[10] L. Máiz Carro, M. Blanco-Aparicio, Nuevos antibióticos inhalados y formas de administración, Open Respir. Arch. 2 (2020) 251–264, https://doi.org/10.1016/j.opresp.2020.05.006.
[11] J.S. Patton, C.S. Fishburn, J.G. Weers, The lungs as a portal of entry for systemic drug delivery, Proc. Am. Thorac. Soc. 1 (2004) 338–344, https://doi.org/10.1513/pats.200409-049TA.
[12] S. Wanning, R. Süverkrüp, A. Lamprecht, Impact of excipient choice on the aerodynamic performance of inhalable spray-freeze-dried powders, Int. J. Pharm. 586 (2020) 119564, https://doi.org/10.1016/j.ijpharm.2020.119564.
[13] P.J. McShane, J.G. Weers, T.E. Tarara, A. Haynes, P. Durbha, D.P. Miller, T. Mundry, E. Operschall, J.S. Elborn, Ciprofloxacin dry powder for inhalation (ciprofloxacin DPI): technical design and features of an efficient drug-device combination, Pulm. Pharm. Ther. 50 (2018) 72–79, https://doi.org/10.1016/j.pupt.2018.03.005.
[14] J.G. Weers, D.P. Miller, T.E. Tarara, Spray-dried PulmoSphere™ formulations for inhalation comprising crystalline drug particles, AAPS PharmSciTech 20 (2019) 103, https://doi.org/10.1208/s12249-018-1280-0.
[15] B. Chaurasiya, Y.-Y. Zhao, Dry powder for pulmonary delivery: a comprehensive review, Pharmaceutics 13 (2021) 31, https://doi.org/10.3390/pharmaceutics13010031.
[16] J. Ling, S. Mangal, H. Park, S. Wang, A. Cavallaro, Q.T. Zhou, Simultaneous particle size reduction and homogeneous mixing to produce combinational powder formulations for inhalation by the single-step co-jet milling, J. Pharm. Sci. 108 (2019) 3146–3151, https://doi.org/10.1016/j.xphs.2019.05.011.
[17] I. Khatib, D. Khanal, J. Ruan, D. Cipolla, F. Dayton, J.D. Blanchard, H.-K. Chan, Ciprofloxacin nanocrystals liposomal powders for controlled drug release via inhalation, Int. J. Pharm. 566 (2019) 641–651, https://doi.org/10.1016/j.ijpharm.2019.05.068.
[18] L.G. Sweeney, Z. Wang, R. Loebenberg, J.P. Wong, C.F. Lange, W.H. Finlay, Spray-freeze-dried liposomal ciprofloxacin powder for inhaled aerosol drug delivery, Int. J. Pharm. 305 (2005) 180–185, https://doi.org/10.1016/j.ijpharm.2005.09.010.
[19] A. Martín, M.J. Cocero, Micronization processes with supercritical fluids: fundamentals and mechanisms, Adv. Drug Deliv. Rev. 60 (2008) 339–350, https://doi.org/10.1016/j.addr.2007.06.019.
[20] C. Costa, T. Casimiro, M.L. Corvo, A. Aguiar-Ricardo, Solid dosage forms of biopharmaceuticals in drug delivery systems using sustainable strategies, Molecules 26 (2021) 7653, https://doi.org/10.3390/molecules26247653.
[21] D.F. Tirado, A. Cabañas, L. Calvo, Modelling and scaling-up of a supercritical fluid extraction of emulsions process, Processes 11 (2023) 1063.
[22] L. Padrela, M.A. Rodrigues, A. Duarte, A.M.A. Dias, M.E.M. Braga, H.C. de Sousa, Supercritical carbon dioxide-based technologies for the production of drug nanoparticles/nanocrystals – a comprehensive review, Adv. Drug Deliv. Rev. 131 (2018) 22–78, https://doi.org/10.1016/j.addr.2018.07.010.
[23] H.K. Ruiz, D.R. Serrano, L. Calvo, A. Cabañas, Current treatments for COVID-19: application of supercritical fluids in the manufacturing of oral and pulmonary formulations, Pharmaceutics 14 (2022) 2380, https://doi.org/10.3390/pr11041063.
[24] F. Zahran, A. Cabanas, J.A. Cheda, J.A. Renuncio, C. Pando, Dissolution rate enhancement of the anti-inflammatory drug diflunisal by coprecipitation with a biocompatible polymer using carbon dioxide as a supercritical fluid antisolvent, J. Supercrit. Fluids 88 (2014) 56–65, https://doi.org/10.1016/j.supflu.2014.01.015.
[25] E. Reverchon, R. Adami, S. Cardea, G.D. Porta, Supercritical fluids processing of polymers for pharmaceutical and medical applications, J. Supercrit. Fluids 47 (2009) 484–492, https://doi.org/10.1016/j.supflu.2008.10.001.
[26] I.A. Cuadra, F. Zahran, D. Martín, A. Cabañas, C. Pando, Preparation of 5-fluorouracil microparticles and 5-fluorouracil/poly (L-lactide) composites by a supercritical CO2 antisolvent process, J. Supercrit. Fluids 143 (2019) 64–71, https://doi.org/10.1016/j.supflu.2014.01.015.
[27] C. Pando, A. Cabañas, I.A. Cuadra, Preparation of pharmaceutical co-crystals through sustainable processes using supercritical carbon dioxide: a review, RSC Adv. 6 (2016) 71134–71150, https://doi.org/10.1039/C6RA10917A.
[28] K. Shi, L. Feng, L. He, H. Li, Solubility determination and correlation of gatifloxacin, enrofloxacin, and ciprofloxacin in supercritical CO2, J. Chem. Eng. Data 62 (2017) 4235–4243, https://doi.org/10.1021/acs.jced.7b00601.
[29] A.I. Caço, F. Varanda, M.J. Pratas de Melo, A.M.A. Dias, R. Dohrn, I.M. Marrucho, Solubility of antibiotics in different solvents. Part II. Non-hydrochloride forms of tetracycline and ciprofloxacin, Ind. Eng. Chem. Res. 47 (2008) 8083–8089, https://doi.org/10.1021/ie8003495.
[30] F. Varanda, M.J. Pratas de Melo, A.I. Caço, R. Dohrn, F.A. Makrydaki, E. Voutsas, D. Tassios, I.M. Marrucho, Solubility of antibiotics in different solvents. 1. Hydrochloride forms of tetracycline, moxifloxacin, and ciprofloxacin, Ind. Eng. Chem. Res. 45 (2006) 6368–6374, https://doi.org/10.1021/ie060055v.
[31] J.W. Ziegler, J.G. Dorsey, T.L. Chester, D.P. Innis, Estimation of liquid-vapor critical loci for CO2-solvent mixtures using a peak-shape method, Anal. Chem. 67 (1995) 456–461, https://doi.org/10.1021/ac00098a034.
[32] G.A. Hebbink, M. Jaspers, H.J.W. Peters, B.H.J. Dickhoff, Recent developments in lactose blend formulations for carrier-based dry powder inhalation, Adv. Drug Deliv. Rev. 189 (2022) 114527, https://doi.org/10.1016/j.addr.2022.114527.
[33] M. Kurakula, G.S.N.K. Rao, Pharmaceutical assessment of polyvinylpyrrolidone (PVP): as excipient from conventional to controlled delivery systems with a spotlight on COVID-19 inhibition, J. Drug Deliv. Sci. Technol. 60 (2020) 102046, https://doi.org/10.1016/j.jddst.2020.102046.
[34] M. Guastaferro, L. Baldino, S. Cardea, E. Reverchon, Supercritical CO2 assisted electrospray of PVP-rutin mixtures using a liquid collector, J. Supercrit. Fluids 188 (2022) 105684, https://doi.org/10.1016/j.supflu.2022.105684.
[35] S. Cardea, E. Reverchon, Supercritical fluid processing of polymers, Polymers 11 (2019), https://doi.org/10.3390/polym11101551.
[36] L. Baldino, S. Cardea, E. Reverchon, Supercritical assisted electrospray: an improved micronization process, Polymers 11 (2019) 244, https://doi.org/10.3390/polym11020244.
[37] A. Pomázi, F. Buttini, R. Ambrus, P. Colombo, P. Szabó-Révész, Effect of polymers for aerolization properties of mannitol-based microcomposites containing meloxicam, Eur. Polym. J. 49 (2013) 2518–2527, https://doi.org/10.1016/j.eurpolymj.2013.03.017.
[38] M. Goyal, G. Tulsyan, D.D. Kanabar, T. Chavan, A. Muth, V. Gupta, Poly vinyl pyrrolidone (PVP) based inhaled delivery carriers for olaparib for non-small cell lung cancer (NSCLC) treatment, J. Drug Deliv. Sci. Technol. 87 (2023) 104767, https://doi.org/10.1016/j.jddst.2023.104767.
[39] I.A. Cuadra, A. Cabañas, J.A. Cheda, F.J. Martínez-Casado, C. Pando, Pharmaceutical co-crystals of the anti-inflammatory drug diflunisal and nicotinamide obtained using supercritical CO2 as an antisolvent, J. CO2 Util. 13 (2016) 29–37, https://doi.org/10.1016/j.jcou.2015.11.006.
[40] I.A. Cuadra, A. Cabañas, J.A. Cheda, M. Túrk, C. Pando, Cocrystallization of the anticancer drug 5-fluorouracil and coformers urea, thiourea or pyrazinamide using supercritical CO2 as an antisolvent (SAS) and as a solvent (CSS), J. Supercrit. Fluids 160 (2020) 104813, https://doi.org/10.1016/j.supflu.2020.104813.
[41] I.I. Hamdan, D. El-Sabawi, R. Darwish, L.A. Dahabiyeh, Preparation, characterization and antimicrobial assessment of selected ciprofloxacin salts, Acta Pharm. 71 (2021) 365–382, https://doi.org/10.2478/acph-2021-0028.
[42] M. Rossmann, A. Braeuer, A. Leipertz, E. Schluecker, Manipulating the size, the morphology and the polymorphism of acetaminophen using supercritical antisolvent (SAS) precipitation, J. Supercrit. Fluids 82 (2013) 230–237, https://doi.org/10.1016/j.supflu.2013.07.015.
[43] I.I. Hamdan, D. El-Sabawi, R. Darwish, L.A. Dahabiyeh, Preparation, characterization and antimicrobial assessment of selected ciprofloxacin salts, Acta Pharm., vol. 71(no. 3921), pp. 365–82. ⟨https://doi.org/10.2478/acph-2021-0028⟩.
[44] O.D. Putra, A. Pettersen, E. Yonemochi, H. Uekusa, Structural origin of physicochemical properties differences upon dehydration and polymorphic transformation of ciprofloxacin hydrochloride revealed by structure determination from powder X-ray diffraction data, CrystEngComm 22 (2020) 7272–7279, https://doi.org/10.1039/D0CE00261E.
[45] Y. Jiang, W. Sun, W. Wang, Recrystallization and micronization of 10-hydroxy-camptothecin by supercritical antisolvent process, Ind. Eng. Chem. Res. 51 (2012) 2596–2602, https://doi.org/10.1021/ie2020334.
[46] A. Montes, L. Wehner, C. Pereyra, E.J. Martínez de la Ossa, Precipitation of submicron particles of rutin using supercritical antisolvent process, J. Supercrit. Fluids 118 (2016) 1–10, https://doi.org/10.1016/j.supflu.2016.07.020.
[47] L. Wu, X. Miao, Z. Shan, Y. Huang, L. Li, X. Pan, Q. Yao, G. Li, C. Wu, Studies on the spray dried lactose as carrier for dry powder inhalation, Asian J. Pharm. Sci. 9 (2014) 336–341, https://doi.org/10.1016/j.ajps.2014.07.006.
[48] D.-S. Lee, H.-J. Han, K. Kim, W.-B. Park, J.-K. Cho, J.-H. Kim, Dissociation and complexation of fluoroquinolone analogues, J. Pharm. Biomed. Anal. 12 (1994) 157–164, https://doi.org/10.1016/0731-7085(94)90025-6.
[49] CRC Handbook of Chemistry and Physics, 1977.
[50] K.P. Basavaraju, S.K. Ranjani, Efficacy of combination of acetic acid and ciprofloxacin eardrops versus only ciprofloxacin eardrops in achieving dry ears in chronic suppurative otitis media, Egypt. J. Otolaryngol. 39 (2023) 106, https://doi.org/10.1186/s43163-023-00466-4.
[51] F. Zahran, J. Morère, A. Cabañas, J.A.R. Renuncio, C. Pando, Role of excess molar enthalpies in supercritical antisolvent micronizations using dimethylsulfoxide as the polar solvent, J. Supercrit. Fluids 60 (2011) 45–50, https://doi.org/10.1016/j.supflu.2011.02.015.
[52] H. Larhrib, G.P. Martin, C. Marriott, D. Prime, The influence of carrier and drug morphology on drug delivery from dry powder formulations, Int J. Pharm. 257 (2003) 283–296, https://doi.org/10.1016/s0378-5173(03)00156-x.
[53] M. Hiroike, J.-i Sakabe, M. Kobayashi, T. Shimauchi, T. Ito, S. Hirakawa, A. Inoh, Y. Tokura, Acicular, but not globular, titanium dioxide nanoparticles stimulate keratinocytes to produce pro-inflammatory cytokines, J. Dermatol. 40 (2013) 357–362, https://doi.org/10.1111/1346-8138.12132.
[54] E.J. Park, T.O. Khaliullin, M.R. Shurin, E.R. Kisin, N. Yanamala, B. Fadeel, J. Chang, A.A. Shvedova, Fibrous nanocellulose, crystalline nanocellulose, carbon nanotubes, and crocidolite asbestos elicit disparate immune responses upon pharyngeal aspiration in mice, J. Immunotoxicol. 15 (2018) 12–23, https://doi.org/10.1080/1547691x.2017.1414339.